

SYNTHESIS OF PROPYLENE FROM ETHANOL USING PHOSPHORUS-MODIFIED HZSM-5

R. S. Costa and M. A. P. da Silva*

Escola de Química, Universidade Federal do Rio de Janeiro, Av. Athos da Silveira Ramos 149,
Bloco E, Ilha do Fundão, CEP: 21941-909, Rio de Janeiro - RJ, Brazil.
Phone: (55) (21) 3938-7606, Fax: (55) (21) 3938-7567
E-mail: monica@eq.ufrj.br

(Submitted: February 26, 2015 ; Revised: June 11, 2015 ; Accepted: June 18, 2015)

Abstract - Effects of phosphorus addition to HZSM-5 on ethanol conversion to propylene were evaluated. Catalysts were characterized by XRF, XRD, nitrogen adsorption, ^{27}Al and ^{31}P MAS NMR, n-propylamine and ammonia TPD. Increasing P content decreased the strength and density of acid total sites. Ethanol dehydration was carried out in a fixed bed reactor operating at atmospheric pressure. Conversion was around 100% for all catalysts. 1.2 wt% of P catalyst showed the highest propylene yield, and was used to evaluate temperature and ethanol partial pressure effects on the product distribution. The highest propylene accumulated productivity was obtained for an ethanol partial pressure of 0.4 atm. Propylene formation was favored in the temperature range 475-500 °C. Significant changes in the product distribution as a function of time on stream were observed at higher temperatures, suggesting stronger catalyst deactivation. The ethylene yield decreased up to 500 °C, rising significantly at 550 °C, possibly due to heavier product cracking reactions.

Keywords: Ethanol; HZSM-5; Phosphorus.

INTRODUCTION

The growing demand for clean and sustainable technologies has led to the development of a new concept known as bioeconomy. In this context bio-refining is defined as the sustainable processing of biomass into a spectrum of marketable products and energy (Morais and Bogel-Lukasik, 2013).

The current availability of bioethanol at low cost and the increasing price of olefins have changed the petrochemical ethylene world scenario. In markets with abundant agricultural resources such as China, Pakistan, India and Brazil, where the petrochemical industry is less developed, ethanol can be used to produce ethylene, propylene, butadiene, and other products (Centi and Santen, 2007). For instance, in Brazil, several industrial plants (Braskem, Dow Brasil and Solvay Indupa Brasil) are producing ethylene via catalytic dehydration of ethanol from fermentation of

sugarcane molasses (Lanzefame *et al.*, 2014).

Light olefins are produced primarily from steam cracking of naphtha and occupy a prominent place in the block of basic or first generation petrochemicals. Their importance is related to their gaseous nature, contributing to integration with other industrial segments, in which second generation petrochemical products (plastics, fibers and intermediates for detergents) are in demand (Tsunoji *et al.*, 2014). Pyrolysis of naphtha is the most widely used process for obtaining a ratio of propylene/ethylene of about 0.5. Therefore, a propylene deficit over time is inevitable. The U.S. Chemical Market Association (CMAI) estimated the annual growth of propylene consumption around 5%. This increase is due to growing demand of polypropylene, acrylonitrile, propylene oxide and other petrochemical products (Nawaz *et al.*, 2009).

An alternative to light olefins production from naphtha is alcoholchemistry, a segment of the chemi-

*To whom correspondence should be addressed

This is an extended version of the work presented at the 20th Brazilian Congress of Chemical Engineering, COBEQ-2014, Florianópolis, Brazil.

cal industry that uses ethanol as a raw material for manufacturing various chemicals (Takahashi *et al.*, 2012).

Development of catalysts and processes to increase the propylene/ethylene ratio is essential to meet the propylene demand. Therefore, the production of propylene from ethanol has attracted considerable attention. The use of zeolites in catalytic conversion of ethanol has been reported by several authors, in particular the use of HZSM-5 for this kind of reaction (Takahashi *et al.*, 2012; Inaba *et al.*, 2006; Lu and Liu, 2011; Barros *et al.*, 2007; Duan *et al.*, 2012; Vu *et al.*, 2010; Song *et al.*, 2010; Ramesh *et al.*, 2009).

The acidity of HZSM-5 leads to a variety of products via oligomerization reactions, particularly aromatic compounds, causing coke deposition and catalyst deactivation (Takahashi *et al.*, 2012; Inaba *et al.*, 2006; Lu and Liu, 2011; Barros *et al.*, 2007; Song *et al.*, 2010; Ramesh *et al.*, 2009). To reduce the density and strength of acid sites of HZSM-5, an increase in SiO₂/Al₂O₃ (Inaba *et al.*, 2006; Song *et al.*, 2010; Blasco *et al.*, 2006), phosphorus addition (Takahashi *et al.*, 2012; Lu and Liu, 2011; Ramesh *et al.*, 2009; Song *et al.*, 2010; Barros *et al.*, 2007; Vu *et al.*, 2010; Zhao *et al.*, 2007) and metals impregnation (Inaba *et al.*, 2006; Blasco *et al.*, 2006) are current alternatives.

The benefits of phosphorus incorporation into HZSM-5 regarding higher selectivity to olefins, and the improving of hydrothermal stability are well established (Takahashi *et al.*, 2012; Lu and Liu, 2011; Ramesh *et al.*, 2009; Song *et al.*, 2010).

The aim of this study was to evaluate the effects of phosphorus incorporation into HZSM-5 on ethanol conversion to light olefins, especially to propylene.

EXPERIMENTAL

A commercial HZSM-5 (SiO₂/Al₂O₃ molar ratio = 24) was impregnated with a phosphoric acid aqueous solution (SIGMA-ALDRICH). This procedure was based on Zhao *et al.* (2007). Water was slowly evaporated from the suspension in a rotary evaporator at 70 °C under vacuum. Then, catalysts were dried at 100 °C for 24 h and calcined at 500 °C (1°C/min) for 1 h. The amount of phosphorus, expressed as weight percent of P, ranged from 0.8 to 3.2. Samples were designated as xPHZSM-5, where *x* is the phosphorus content (wt %).

The chemical composition of catalysts was evaluated by X-ray fluorescence (XRF) using a Rigaku RIX 3100 spectrometer. Catalyst textural properties were quantified by physical adsorption of N₂ at -196 °C on a Micromeritics TriStar 3000 equipment. Samples

were pretreated at 300 °C under vacuum for 18 h. X-ray diffraction (XRD) patterns were obtained with a diffractometer (Rigaku Miniflex) using CuK α radiation ($\lambda = 1.5417 \text{ \AA}$, 30 kV, 15 mA, 0.05 °/s).

Temperature programmed desorption of n-propylamine (n-propylamine-TPD) was carried out in a TPD/TPR 2900 (Micromeritics) equipment, coupled to a mass spectrometer model OMNISTAR™ 422 (Pfeiffer). The catalysts were pretreated *in situ* at 500 °C (10 °C/min) for 1 h with He. The sample was then exposed to pulses of n-propylamine in He at room temperature. After saturation, samples were submitted to helium flow (20 mL/min) for 30 min at room temperature and then heated up to 200 °C at a heating rate of 5 °C/min under the same flow rate of helium in order to remove physisorbed n-propylamine. Finally, the n-propylamine-TPD experiment was carried out in the range 200-500 °C (5 °C/min) and kept at this temperature for 2 h using He (20 mL/min). The mass fragment $m/e = 41$ (propylene) was analyzed.

Analysis of the temperature programmed desorption of ammonia (NH₃-TPD) was carried out in a multipurpose unit. The sample was pretreated in flowing He (30 mL/min) at 500 °C (10 °C/min) for 1 hour. Then temperature was lowered to 100 °C and treated with a 4% mixture of NH₃/He (30 mL/min) during 30 min. After NH₃ adsorption, the sample was flushed with He (30 mL/min) for 30 min at 100 °C. Finally, the NH₃-TPD experiment was carried out in the range of 100- 800 °C (5 °C/min) using He (30 mL/min). The mass fragment $m/e = 15$ was analyzed by a mass spectrometer.

Solid-state magic angle spinning nuclear magnetic resonance (MAS NMR) experiments were performed on a Bruker Avance 400 spectrometer, at room temperature and 9.4 Tesla. ²⁷Al MAS NMR and ³¹P MAS NMR spectra were obtained at 15 and 14 kHz, respectively. Each ²⁷Al spectrum resulted from 2048 scans, at intervals of 0.5 s; each ³¹P spectrum resulted from 128 scans, at intervals of 60 s. The ²⁷Al chemical shifts were referenced to Al(H₂O)₆³⁺ while the ³¹P were referenced to an aqueous solution of H₃PO₄ (85%).

Catalytic reactions were carried out in a fixed bed tubular reactor, operating at atmospheric pressure. Catalysts were pretreated *in situ* under He (30 mL/min) for 1h at 500 °C. Ethanol (SIGMA-ALDRICH 99.8%) was pumped to the vaporizer at 200 °C by a syringe pump (BBRAUN) and mixed with He at a total flow rate of 40 mL/min. To investigate the effects of time on stream upon ethanol conversion, the reaction was carried out at 500 °C for 228 min. The effects of phosphorus addition, ethanol partial pressure (0.1-0.4 atm) temperature (450-500 °C) were also evaluated. The operating conditions used aimed to increase pro-

pylene yield as suggested by Schulz and Bander-mann (1994), Inaba *et al.* (2006), Song *et al.* (2010) and Duan *et al.* (2012).

Samples of reactor effluent were taken after the first 15 min of reaction and, afterwards, in intervals of 71 min. The reactor effluent was analyzed online by an Agilent 6890 gas chromatograph equipped with flame ionization and thermal conductivity detectors, using a HP-PLOT/Q column (30 m, 0.53 mm).

The yield (Y_i) of products and the instantaneous productivity of propylene (IPP) were calculated by the following equations:

$$Y_i = \frac{\text{mass of ethanol consumed to form the product } i}{\text{mass of fed ethanol}} \quad (1)$$

$$\text{IPP} = Y_p E_{\text{WHSV}} f M_p / M_E \quad (2)$$

where E_{WHSV} represents the space velocity of ethanol and was defined as the ratio of the mass flow rate of ethanol to catalyst mass, Y_p is the propylene yield, f is the stoichiometric molar ratio of propylene to ethanol (2/3), M_p is the molar mass of propylene, and M_E is the molar mass of ethanol.

RESULTS AND DISCUSSION

Catalyst Characterization

The chemical composition, the relative crystallinity and the textural properties of the calcined catalysts are listed in Table 1.

As shown, the P content of HZSM-5 is approximately the aimed value. XRD profiles (Figure 1), suggest that parent HZSM-5 sample was a typical material corresponding to the MFI structure and no additional phases were found for all catalysts. Addition of phosphorus caused a slight reduction on relative crystallinity. This decreased XRD crystallinity could be due to framework defects caused by dealumination as reported in literature (Tavan *et al.*, 2014; Lu and Liu, 2011; Zhao *et al.*, 2007).

Textural properties of catalysts showed that specific surface area, micropore area and micropore volume decreased with the increase in phosphorus content. This effect could be associated to formation of species containing phosphorus which would block or destroy the porous structure of zeolite. Our results confirm the findings of Gou *et al.* (2014), Tavan *et al.* (2014), Hodala *et al.* (2014), Ramesh *et al.* (2009), Blasco *et al.* (2006), Barros *et al.* (2007) and Zhao *et al.* (2007).

Table 1: Chemical composition, relative crystallinity and textural properties of catalysts.

Catalyst	Chemical composition		XRD ^a (%)	Textural properties		
	P (wt %)	P/Al (mol/mol)		Specific area (m ² /g) ^(b)	Micropore area (m ² /g) ^(c)	Micropore volume (cm ³ /g) ^(c)
HZSM-5	-	-	100	370	273	0.126
0.8PHZSM-5	0.8	0.2	100	358	256	0.118
1.2PHZSM-5	1.2	0.3	94.4	340	247	0.114
3.2PHZSM-5	3.2	0.8	84.8	253	196	0.091

^a relative crystallinity; ^b BET method; ^c t-plot method

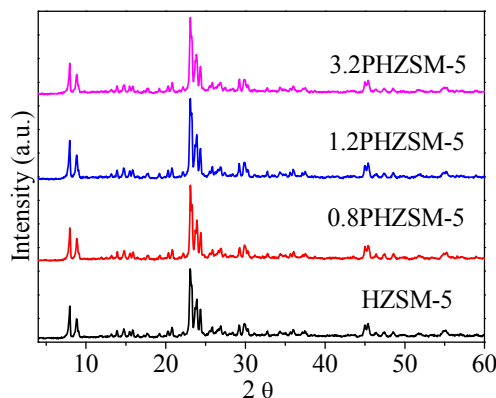


Figure 1: XRD profiles of calcined catalyst.

NH₃-TPD profiles of the parent HZSM-5 and P-modified HZSM-5 samples are shown in Figure 2. All samples showed three desorption peaks: the first one at temperatures lower than 310 °C (weak acid sites), the second at temperatures between 310 and 590 °C (moderate strength acid sites) and the third peak at temperatures higher than 590 °C (strong acid sites).

Furthermore, Figure 2 shows that the desorption peaks shifted slightly to lower temperatures as the phosphorus content increased, suggesting that the strength and total acid site density decreased, especially the strong ones. Similar results were reported in the literature (Hodala *et al.*, 2014; Takahashi *et al.*, 2012; Lu and Liu, 2011; Song *et al.*, 2010; Vu *et al.*, 2010; Li *et al.*, 2010; Ramesh *et al.*, 2009; Zhao *et al.*, 2007; Lercher and Rumpelmayr, 1986). The addition of P up to 1.2 wt. % decreased the strength of weak and strong acid sites, while the addition of 3.2 wt. % decreased markedly the strength of strong acid sites. The total density of acid sites slowly decreased up to 0.8 wt.% of P, but this reduction was more pronounced for higher phosphorous content. The

addition of 1.2 wt. % of P reduced the total acid site density by approximately 64 %, while for 3.2PHZSM-5 the reduction was around 80% as compared to HZSM-5 (see Table 2). These results are similar to those of Caeiro *et al.* (2006) and Lu and Liu (2011). Hodala *et al.* (2014) verified by TPD-NH₃ that stronger acid sites were replaced with weaker ones after phosphate modification.

Figure 3 shows n-propylamine-TPD profiles of the calcined catalysts. This technique is used for measuring the Brønsted acid density and is based on formation of alkylammonium ions (from adsorbed alkyl amines that are protonated by Brønsted sites) which decompose to ammonia and olefins in a well-defined temperature range via a reaction similar to the Hofmann-elimination (Kresnawahjuesa *et al.*, 2002).

According to Figure 3, Brønsted acidity decreases with the addition of phosphorus. Ramesh *et al.* (2009) reported that impregnation of H₃PO₄ on HZSM-5 promotes modification of surface acidity, decreasing density and strength of acid sites. This modification of surface acidity can be attributed to a partial dealumination and/or formation of species P-O-Al.

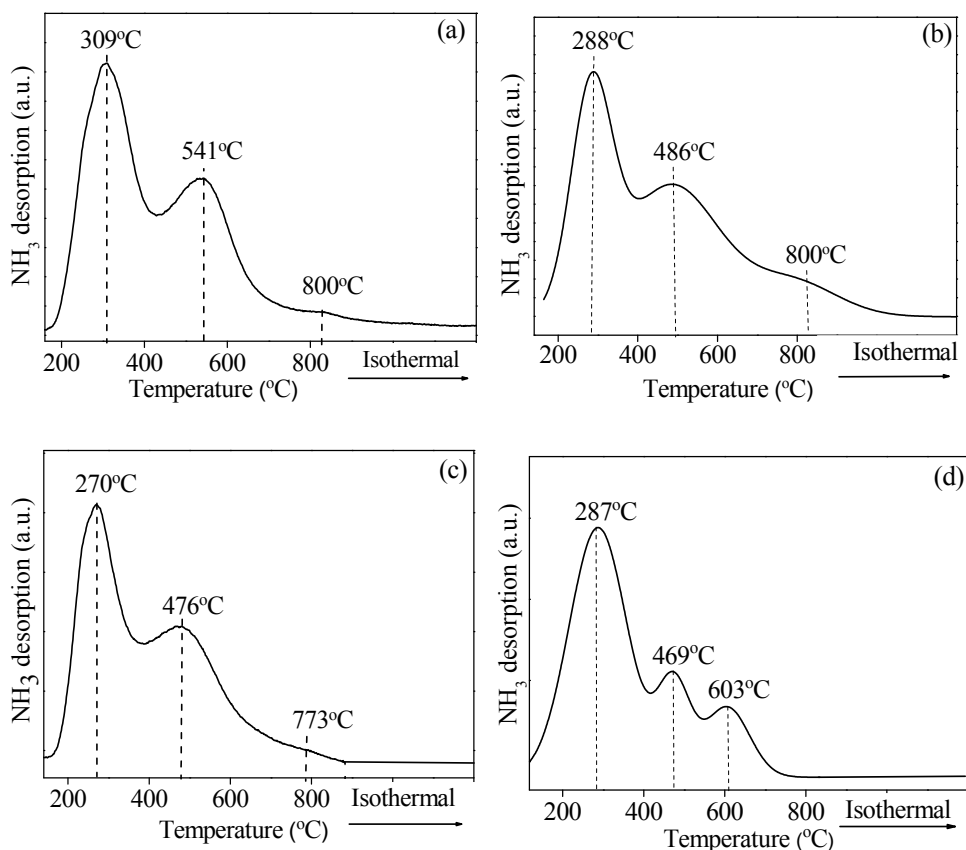


Figure 2: NH₃-TPD profiles of HZSM-5 (a), 0.8PHZSM-5 (b), 1.2PHZSM-5 (c) and 3.2PHZSM-5(d)

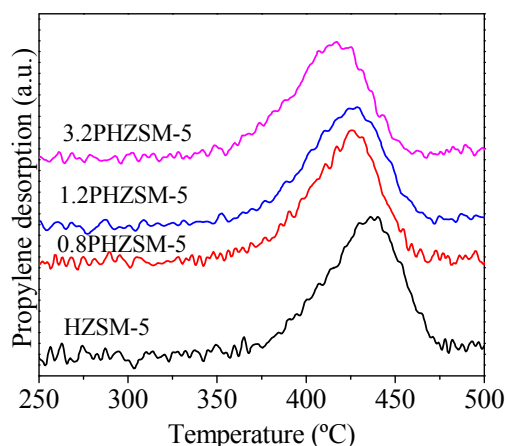


Figure 3: Calcined catalysts n-propylamine-TPD profiles.

The catalysts' acid properties measured by NH_3 -TPD and n-propylamine-TPD are listed in Table 2. Phosphorus addition to HZSM-5 caused a decrease in the total acid site density. It also appears that the decrease in strong acid sites density was greater than that observed for weak acid sites, as reported previously (Takahashi *et al.*, 2012; Lu and Liu, 2011; Ramesh *et al.*, 2009; Song *et al.*, 2010; Vu *et al.*, 2010; Li *et al.*, 2010; Zhao *et al.*, 2007; Lercher and Rumplmayr, 1986).

Phosphorous loading of HZSM-5 decreased the total density of acid sites as well as their acid strength (Takahashi *et al.*, 2012; Lu and Liu, 2011; Ramesh *et al.*, 2009; Song *et al.*, 2010; Barros *et al.*, 2007; Lecher and Rumplmayr, 1986). Note that the total density of acid sites measured by NH_3 -TPD decreased significantly with P addition. However, the addition of phosphorus resulted in a minor modification in the density of Brønsted acid sites.

Lercher and Rumplmayr (1986) showed that adding H_3PO_4 to HZSM-5 might convert strong

Brønsted acid sites to weak ones, without altering the acid-base properties in general. However, Lischke *et al.* (1991) reported a decrease in the density of Brønsted acid sites as a result of interaction of H_3PO_4 with the framework hydroxyl groups of HZSM-5.

Figure 4 shows ^{27}Al MAS NMR spectra of HZSM-5 and phosphorus modified HZSM-5 (xPHZSM-5). The spectrum of the calcined parent zeolite presents two peaks. The intense peak at 60 ppm is ascribed to tetrahedral Al species (Al_{tet}) inside the zeolite framework, and another one at 3.4 ppm is typical of extra-framework octahedral Al species (Al_{oct}), as reported by Zhao *et al.* (2007) and Blasco *et al.* (2006). Similar spectra are obtained for the xPHZSM-5 catalysts, but the peak of Al_{oct} appears now in the region of -3 and -7 ppm. A broad peak becomes evident at 36-40 ppm, related to distorted tetrahedral aluminum species ($\text{Al}_{\text{dist-tet}}$) and/or penta-coordinated aluminum. Gou *et al.* (2014), Zhao *et al.* (2007) and Blasco *et al.* (2006) also observed these peaks.

Table 2: Acid properties of calcined catalysts.

Catalyst	Total acid ($\mu\text{mol}/\text{m}^2$)	Total acid ($\mu\text{mol}/\text{g}$)	Acid strength distribution ($\mu\text{mol}/\text{g}$ [%])			Brønsted acid ($\mu\text{mol}/\text{m}^2$)	Brønsted acid ($\mu\text{mol}/\text{g}$)
			Weak $T \leq 310$ °C	Moderate $310-590$ °C	Strong $T \geq 590$ °C		
HZSM-5	5.33	1971	507 [26]	1132 [57]	331 [17]	0.98	364.5
0.8PHZSM-5	4.56	1631	463 [28]	670 [41]	499 [31]	0.95	339.5
1.2PHZSM-5	1.94	661	361 [55]	269 [41]	31 [5]	0.93	315.9
3.2PHZSM-5	1.51	382	167 [44]	177 [46]	38 [10]	1.17	294.9

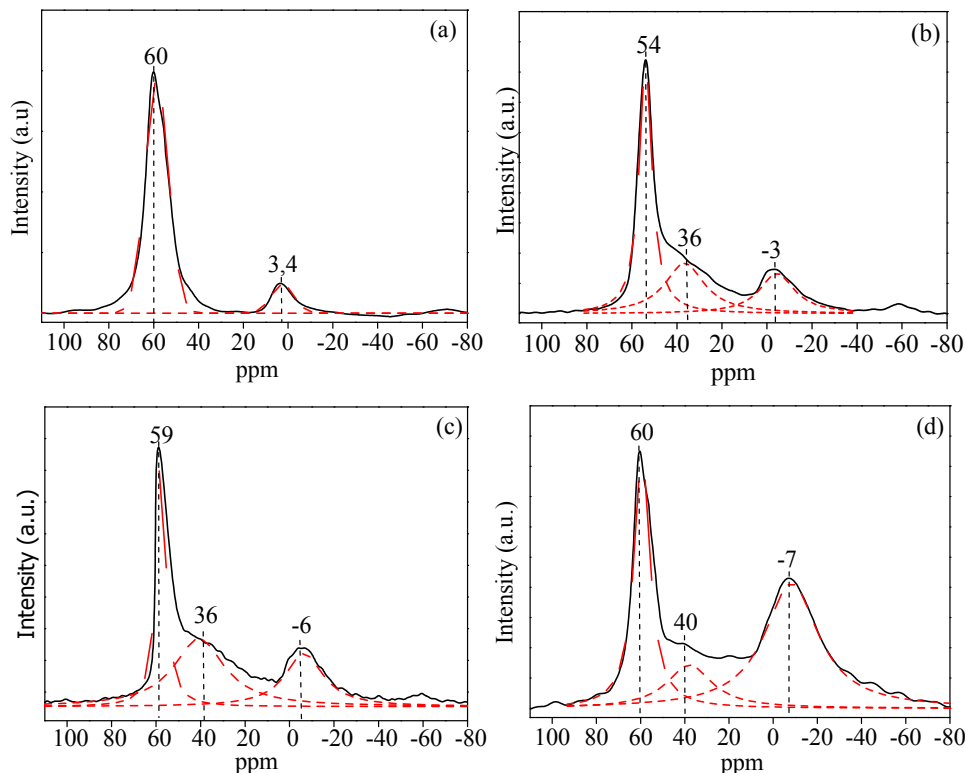


Figure 4: ^{27}Al MAS NMR spectra of HZSM-5 (a), 0.8PHZSM-5 (b), 1.2PHZSM-5 (c) and 3.2PHZSM-5 (d).

Table 3 shows relative percentage of peaks present in the ^{27}Al MAS NMR indicating that the relative intensities of Al_{oct} increased as the concentration of phosphorus added to HZSM-5 increased; this behavior was also observed by Zhao *et al.* (2007). However, for $\text{Al}_{\text{dist-tet}}$, the intensity increased up to the catalyst with 1.2% P and then decreased. It can be seen that the framework SAR (SAR_f) increases with increasing phosphorus concentration added to the HZSM-5. Partial dealumination of the HZSM-5 framework is due to phosphorus modification. However, according to Gou *et al.* (2014) the extra-framework aluminum species can be transformed in aluminum phosphates by interacting with phosphorus.

Table 3: Relative percentage of peaks present in the ^{27}Al MAS NMR.

Catalyst	Al_{tet} (%)	$\text{Al}_{\text{dist-tet}}$ (%)	Al_{oct} (%)	SAR_f
HZSM-5	89	-	11	27
0.8PHZSM-5	52	28	20	45
1.2PHZSM-5	46	31	23	52
3.2PHZSM-5	31	16	53	77

According to the results, a linear relationship between Al_{tet} and acidity measured by n-propylamine-

TPD (Figure 5) was obtained, agreeing with Caeiro *et al.* (2006) and Menezes *et al.* (2006).

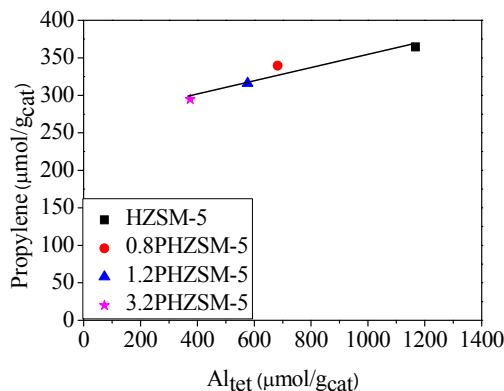


Figure 5: Relationship between Brønsted acidity expressed as μmol of propylene/ g_{cat} and Al_{tet} concentration.

Ramesh *et al.* (2009) reported that tetrahedral aluminum is the main species responsible for surface acidity of zeolite. This means that framework tetrahedral aluminum is responsible for the surface acidity of HZSM-5. Caeiro *et al.* (2006) also correlated Al_{tet} with the Brønsted acidity present in the

zeolite. However, phosphorus addition to zeolite increases the concentration of $\text{Al}_{\text{dist-tet}}$, which can also contribute to the zeolite acidity.

^{31}P MAS NMR spectra of calcined catalysts are illustrated in Figure 6.

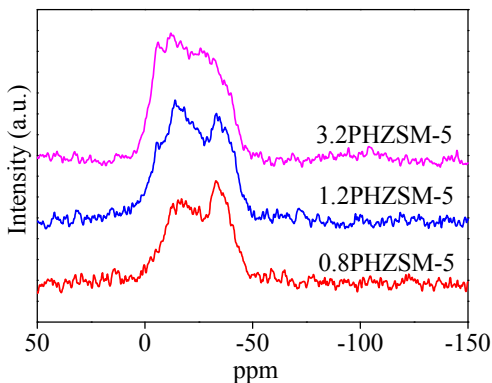


Figure 6: ^{31}P MAS NMR spectra of calcined catalysts.

Intense peaks are observed between 0 and -13 ppm. These can be attributed to P in pyrophosphoric acid, pyrophosphate or short chain polyphosphates. However, Blasco *et al.* (2006) attributed the -13 ppm signal to intermediate groups in short chain polyphosphates or polyphosphates attached to Al (Ramesh *et al.*, 2009; Caeiro *et al.*, 2006). According to Ramesh *et al.* (2009), such polyphosphates could be responsible for blocking the pores of ZSM-5. This would explain the decrease of specific surface area with phosphorus addition to HZSM-5 (Table 1).

Peaks observed between -25 and -35 ppm were assigned to amorphous aluminum phosphate or monomeric phosphate. The signal at -30 ppm was attributed to AlPO_4 or $(\text{SiO})_x\text{Al}(\text{OP})_{4-x}$ species and the increase in phosphorus content raised the peak intensity of pyrophosphoric acid, as reported by Blasco *et al.* (2006) and Zhao *et al.* (2007).

Catalytic Tests

In most cases, conversion of ethanol was around 100% for all catalysts, but the product distribution depended on the content of phosphorus (Takahashi *et al.*, 2012; Lu and Liu, 2011; Song *et al.*, 2010). Ethanol was converted to ethylene, propylene, $\text{C}_1\text{-C}_3$ paraffins, hydrocarbons with 4 carbons, hydrocarbons with 5 carbons and hydrocarbons with more than 6 carbons.

Figure 7 presents the instantaneous productivity of propylene (IPP) as a function of time on stream (TOS) at 500 °C with an ethanol partial pressure of 0.4 atm for calcined catalysts.

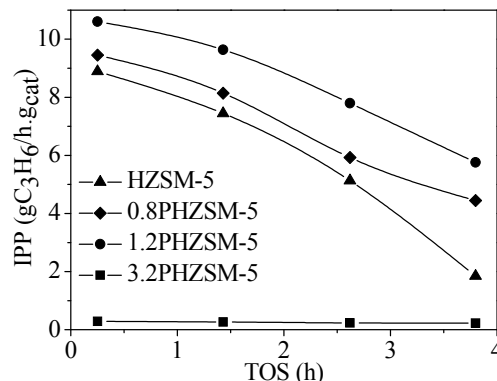


Figure 7: Instantaneous productivity of propylene (500 °C; $p_{\text{EtOH}} = 0.4$ atm; $g_{\text{cat}} = 0.025$ g; total flow rate = 40 mL/min).

As shown, the instantaneous productivity of propylene increased with higher P contents, reaching a maximum value at 1.2 wt %, and then decreasing sharply. Besides that, catalysts 1.2PHZSM-5 and HZSM-5 presented, respectively, the lower and higher sensitivity over time. 3.2 wt % of P practically suppressed the formation of propylene. These results suggest that acidity plays an important role in the formation of propylene and that moderate surface acidity is fundamental to increase its productivity (Barros *et al.*, 2007, Song *et al.*, 2010).

According to Inaba *et al.* (2006), ethylene and C_4 olefins formed by ethanol dehydration at elevated temperatures can favor other reactions such as oligomerization, aromatization, hydrogen transfer or cracking reactions to form propylene, butenes and higher paraffins. Song *et al.* (2010) concluded that these reactions are promoted by strong acid sites and that a decrease of acidity by added phosphorus directly affects the density of sites, increasing the yield of lights olefins.

Takahashi *et al.* (2012) evaluated the effects of phosphorus incorporation to HZSM-5 ($\text{SiO}_2/\text{Al}_2\text{O}_3 = 80$) on ethanol conversion at 550 °C. They found that a catalyst with $\text{P}/\text{Al} = 0.5$ presented the highest yield in propylene. For higher values of P/Al , the propylene yield decreased gradually. Lu and Liu (2011) also investigated the effects of phosphorus on HZSM-5 ($\text{SiO}_2/\text{Al}_2\text{O}_3 = 20$). They obtained the highest yield of propylene for $\text{P}/\text{Al} = 0.95$. For higher values of P/Al , propylene and ethylene yield decreased and increased, respectively, at 450 °C.

In the present work the catalyst 1.2PHZSM-5 ($\text{P}/\text{Al} = 0.3$) was the most stable under all conditions, attesting that incorporation of P to HZSM-5 increases its hydrothermal stability and reduces the formation of coke, in agreement with Takahashi *et*

al. (2012), Lu and Liu (2011), Song *et al.* (2010) and Ramesh *et al.* (2009).

It is worth mentioning that the best P/Al ratio for the formation of propylene differs from one work to another since it depends on experimental conditions such as temperature, ethanol partial pressure, space velocity and type of phosphorus precursor used in the impregnation. Lu and Lui (2011) and Takahashi *et al.* (2012) used, respectively, $(\text{NH}_4)_3\text{PO}_4$, and $(\text{NH}_4)_2\text{HPO}_4$ as phosphorous precursors, while in this work H_3PO_4 was used as a precursor. Blasco *et al.* (2006) reported that the decrease in acidity of ZSM-5 was stronger for the samples modified with H_3PO_4 as compared to samples modified by $\text{NH}_4\text{H}_2\text{PO}_4$ for the same ratio P/Al.

Another concern of this work regarded the effects of ethanol partial pressure on ethanol conversion and the product distribution over 1.2PHZSM-5. Figure 8 illustrates this fact as a function of ethanol partial pressure for 1.2PHZSM-5 after 15 and 228 minutes of reaction, respectively. For the first 15 minutes, an increase in ethanol partial pressure favored the formation of propylene and other products from hydrogen transfer and oligomerization reactions. After 228 minutes, for ethanol partial pressure values above 0.2 atm, the propylene yield stabilized around 12%.

Schulz and Bandermann (1994) studied the effects of ethanol partial pressure on the product distribution over HZSM-5 and found that an increase in ethanol partial pressure decreased the yield of olefins while increasing that of aromatic compounds. Similar results can be observed in Figure 8(b).

Figure 9 illustrates the product distribution as a function of temperature after 15 and 228 minutes, respectively. Figure 9(a) shows that, for 15 minutes, the propylene yield increased slightly with increasing temperature up to 500 °C, decreasing at higher temperatures. However, the ethylene yield de-

creased with increasing temperature up to 500 °C, then increased for higher temperatures. As shown in Figure 9(b), at 550 °C the main product was ethylene, while other products decreased over time. The most significant change in the product distribution versus time was observed at 550 °C, suggesting that at this temperature more intense catalyst deactivation occurred.

According to Song *et al.* (2010), ethanol conversion to propylene is promoted by oligomerization, hydrogen transfer, isomerization and aromatization reactions. However, a temperature increase favors the formation of long chain products from propylene, decreasing its concentration. Ethylene is clearly the only product observed at 400 °C because, at this temperature, ethylene is formed by ethanol intramolecular dehydration (Inaba *et al.*, 2006). However, the increase in ethylene yield at 550 °C is due to the secondary cracking reactions, which are favored at higher temperatures, where the long chain compounds are able to form lighter ones. This behavior was also observed by Duan *et al.* (2012).

Figure 10 shows the profiles of the cumulative amount of propylene (CAP) formed as a function of cumulative amount of fed ethanol (CAFE) for 1.2PHZSM-5 with different ethanol partial pressures in the range of 450 to 550 °C. The dashed lines in Figure 10 correspond to extrapolations based on exponential functions fitted to the data. This strategy enabled the comparison of the cumulative amount of propylene formed and fed ethanol, for each diagram shown.

According to these results, an ethanol partial pressure of 0.4 atm shows the highest CAP for all temperatures, except for 450 °C, at which CAP was favored by an ethanol partial pressure of 0.1 atm. The CAP values at 475 and 500 °C at a partial pressure of 0.4 atm were very near, but the greatest value occurred at 500 °C.

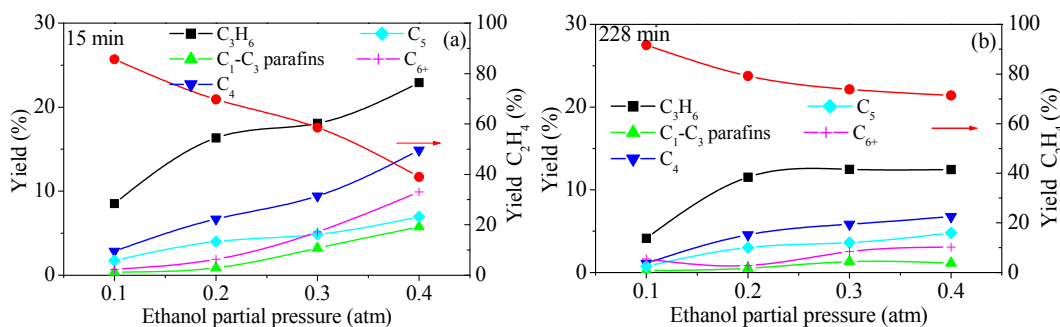


Figure 8: Distribution of products as function of the ethanol partial pressure, 1.2PHZSM-5: (a) after 15 min, (b) after 228 min (500 °C; $g_{\text{cat}} = 0.025\text{g}$; total flow rate = 40mL/min).

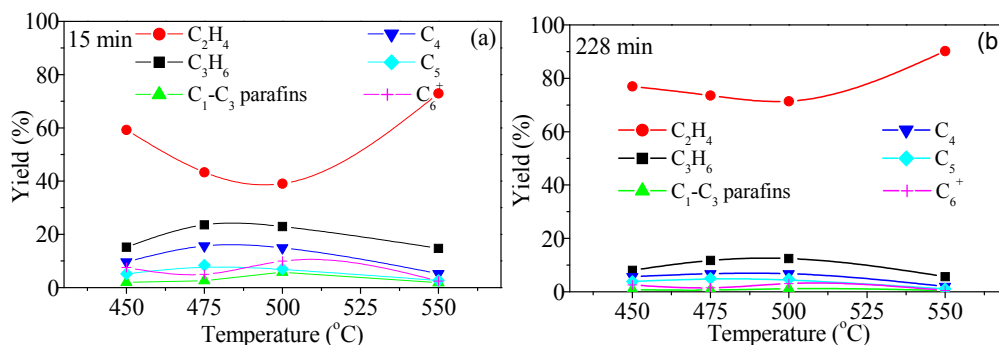


Figure 9: Distribution of products as a function of temperature, 1.2PHZSM-5: (a) after 15 min, (b) after 228 min ($p_{EtOH} = 0.4$ atm; $g_{cat} = 0.025$ g; total flow rate = 40mL/min).

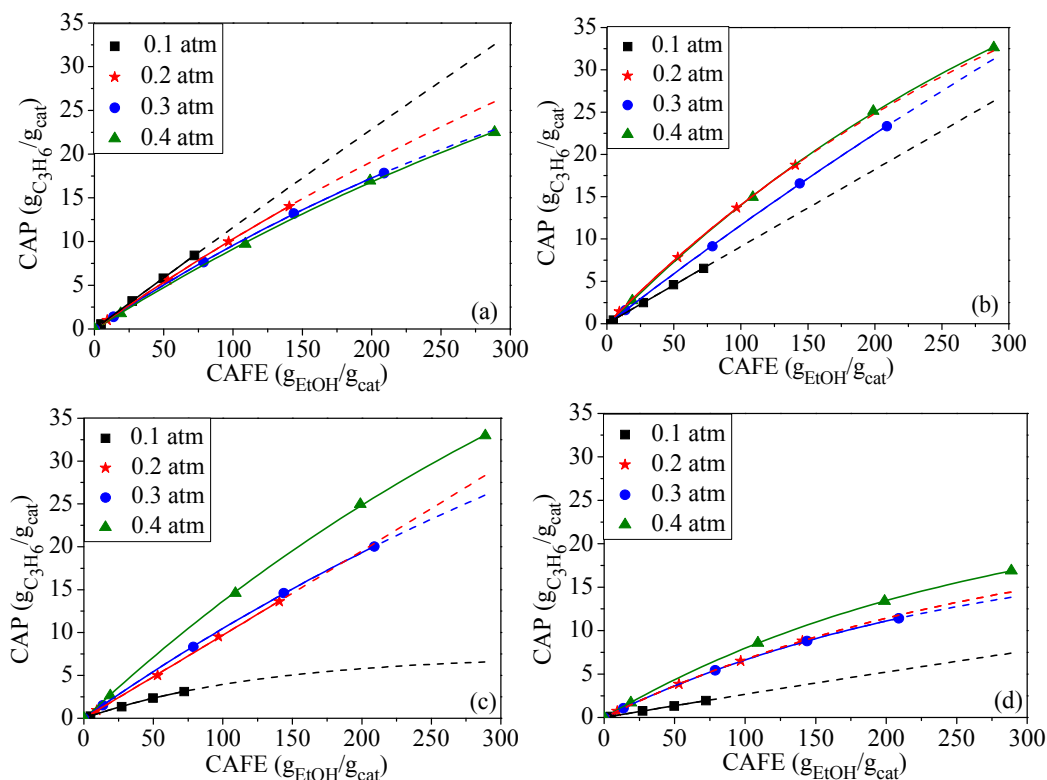


Figure 10: Cumulative amount of propylene formed versus cumulative amount of fed ethanol for 1.2PHZSM-5: (a) 450 °C, (b) 475 °C, (c) 500 °C (d) 550 °C, ($g_{cat} = 0.025$ g; total flow rate = 40 mL/min)

CONCLUSIONS

In evaluating the effect of adding phosphorus to HZSM-5, one observes the reduction of specific area and of density of total acid sites and Brönsted sites. The increase in concentration of Al_{oct} and $Al_{dist-tet}$ as a function of phosphorus addition to HZSM-5 was

established. The ^{31}P MAS NMR analysis showed that the concentration of pyrophosphate increased with increasing phosphorus content, while the concentration of polyphosphates decreased. A linear relationship between Brönsted acidity expressed as μmol propylene/ g_{cat} and the amount of Al_{tet} , which depends on the phosphorous content, was observed. The

content of phosphorus incorporated into HZSM-5 affected the productivity of propylene and the best performance was achieved for the 1.2PHZSM-5. The catalyst 3.2PHZSM-5 presented the lowest productivity in propylene due to its reduced acidity, favoring only ethanol dehydration. The increase of ethanol partial pressure favored the formation of propylene under the tested conditions. Regarding the effect of temperature on ethanol conversion over 1.2PHZSM-5, it was concluded that, for temperatures close to 400 °C the intramolecular dehydration of ethanol is favored, giving predominantly ethylene. Propylene yield reached its maximum in the range of 475-500 °C and at 550 °C the formation of ethylene was prioritized due to secondary cracking reactions at high temperatures. On the basis of the results achieved in this work, and restricted to the operational conditions used therein, the following strategy would maximize the propylene production: ethanol space velocity, 76 g_{EtOH}/(g_{cat} h), 500 °C and P/Al (0.3) molar ratio.

ACKNOWLEDGEMENTS

The authors acknowledge, NUCAT/PEQ/COPPE/UFRJ, Laboratório Multiusuário RMN de sólidos/IQ/UFRJ and GreenTec/EQ/UFRJ for characterization analyses of the catalysts.

REFERENCES

- Barros, Z. S., Zotin, F. M. Z. and Henriques, C. A., Conversion of natural gas to higher valued products: Light olefins production from methanol over ZSM-5 zeolites. *Stud. Surf. Sci. Catal.*, 67, 255 (2007).
- Blasco, T., Corma, A. and Martinez-Triguero, J., Hydrothermal stabilization of ZSM-5 catalytic-cracking additives by phosphorus addition. *J. Catal.*, 237, 267 (2006).
- Caeiro, G., Maagnoux, P., Lopes, J. M., Ramôa Ribeiro, F., Menezes, S. M. C., Costa, A. F. and Cerqueira, H. S., Stabilization effect of phosphorus on steamed H-MFI zeolites. *Appl. Catal.*, A, 314, 160 (2006).
- Centi, G. and Santen R. A., *Catalysis for Renewables*. S. Pariente, N. Tanchoux, F. Fajula, G. Centi, S. Perathoner, Ed., Wiley-VCH Verlag GmbH and Co. KGaA, Weinheim, 9, p. 183-205 (2007).
- Duan, C., Zhang, X., Zhou, R., Hua, Y., Zhang, L. and Chen, J., Comparative studies of ethanol to propylene over HZSM-5/SAPO-34 catalysts prepared by hydrothermal synthesis and physical mixture. *Fuel Process. Technol.*, 108, 31 (2012).
- Gou, M-L., Wang, R., Qiao, Q. and Yang, X., Effect of phosphorus on acidity and performance of HZSM-5 for the isomerization of styrene oxide to phenylacetaldehyde. *Appl. Catal.*, A, 482, 1 (2014).
- Hodala, J. H., Halgeri, A. B. and Shanbhag, G. V., Phosphate modified ZSM-5 for the shape selective synthesis of *para*-diethylbenzene: Role of crystal size and acidity. *Appl. Catal.*, A, 484, 8 (2014).
- Inaba, M., Murata, K., Saito, M. and Takahara, I., Ethanol conversion to aromatic hydrocarbons over several zeolite catalysts. *React. Kinet. Catal. Lett.*, 88(1), 135 (2006).
- Kresnawahjuesa, O., Gorte, R. J., Oliveira, D. and Lau, L. Y., A simple, inexpensive, and reliable method for measuring Brønsted-acid site densities in solid acids. *Catal. Lett.*, 82, 155 (2002).
- Lanzafame, P., Centi, G., Siglinda, P., Evolving scenarios for biorefineries and the impact on catalysis. *Catal. Today*, 234, 2 (2014).
- Lercher, J. A. and Rumpelmayr, G., Controlled decrease of acid strength by orthophosphoric acid on ZSM5. *Appl. Catal.*, A, 25, 215 (1986).
- Li, P., Zhang, W., Han, X. and Bao, Xi., Conversion of methanol to hydrocarbons over phosphorus-modified ZSM-5/ZSM-11 intergrowth zeolites. *Catal. Lett.*, 134, 124 (2010).
- Lischke, G., Eckelt, R., Jerschke, H.-G., Parltitz, B., Schreier, E., Storek, W., Zibrowius, B. and Ohlmann, G., Spectroscopic and physicochemical characterization of P-modified H-ZSM-5. *J. Catal.*, 132, 229 (1991).
- Lu, J. and Liu, Y. J., Effects of P content in a P/HZSM-5 catalyst on the conversion of ethanol to hydrocarbons. *J. Natural Gas Chem.*, 20, 162 (2011).
- Menezes, S. M. C., Lam, Y. L., Damodaram, K. and Ppruski, M., Modification of H-ZSM-5 zeolites with phosphorus. 1. Identification of aluminum species by ²⁷Al solid-state NMR and characterization of their catalytic properties. *Microporous Mesoporous Mater.*, 95, 286 (2006).
- Morais, A. R. C., Bogel-Lukasik, R., Green chemistry and the biorefinery concept. *Sustain. Chem. Process*, 1(18), 1 (2013).
- Nawaz, Z., Tang, X. and Wei, F., Hexene catalytic cracking over 30% SAPO-34 catalyst for propylene maximization: Influence of reaction conditions and reaction pathway exploration. *Braz. J. Chem. Eng.*, 26, 705 (2009).
- Ramesh, K., Hui, L. M., Han, Y. and Borgna, A., Structure and reactivity of phosphorous modified H-ZSM-5 catalysts for ethanol dehydration. *Catal. Comun.*, 10, 567 (2009).

- Schulz, J. and Bandermann, F., Conversion of ethanol over zeolite H-ZSM-5. *Chem. Eng. Technol.*, 17, 179 (1994).
- Song, Z., Takahashi, A., Nakamura, I. and Fujitani, T., Phosphorus-modified ZSM-5 for conversion of ethanol to propylene. *Appl. Catal., A*, 384, 201 (2010).
- Takahashi, A., Xia, W., Nakamura, I., Shimada, H. and Fujitani, T., Effects of added phosphorus on conversion of ethanol to propylene over ZSM-5 catalysts. *Appl. Catal., A*, 423-424, 162 (2012).
- Tavan, Y., Nikou, M. R. K. and Shariati, A., Effect of the P/Al ratio on the performance of modified HZSM-5 for methanol dehydration reaction. *J. Ind. Eng. Chem.*, 20, 668 (2014).
- Tsunoji, N., Sonoda, T., Furumoto, Y., Sadakene, M. and Sano, T., Recreation of Brønsted acid sites in phosphorus-modified HZSM-5(Ga) by modification with various metal cations. *Appl. Catal., A*, 481, 161 (2014).
- Vu, D. V., Hirota, Y., Nishiyama, N., Egashira, Y. and Ueyama, K. J., High propylene selectivity in methanol-to-olefin reaction over H-ZSM-5 catalyst treated with phosphoric acid. *J. Jpn. Petrol. Inst.*, 53, 232 (2010).
- Zhao, G., Teng, J., Xie, Z., Jin, W., Yang, W. and Chen, Q., Effect of phosphorus on HZSM-5 catalyst for C4-olefin cracking reactions to produce propylene. *J. Catal.*, 248, 29 (2007).